PROTEINS
STRUCTURE ■ FUNCTION ■ BIOINFORMATICS

STRUCTURE NOTE

Crystal structure of the dimerization domain of human filamin A

Min-Duk Seo,[1†] Seung-Hyeon Seok,[1†] Hookang Im,[1] Ae-Ran Kwon,[1] Sang Jae Lee,[2] Hyung-Ryong Kim,[3] Yongcheol Cho,[4] Dongeun Park,[4] and Bong-Jin Lee[1*]

[1] Research Institute of Pharmaceutical Sciences, College of Pharmacy, Seoul National University, Seoul 151-742, Korea

[2] Promeditech Ltd., Seoul 151-010, Korea

[3] Department of Dental Pharmacology, School of Dentistry, Wonkwang University, Iksan, Chonbuk 570-749, Korea

[4] School of Biological Sciences, Seoul National University, Seoul 151-742, Korea

Key words: filamin A; domain 24; immunoglobulin-like fold; dimerization interface; crystal structure.

INTRODUCTION

Reorganization of actin cytoskeleton plays a central role in many cell functions such as the maintenance of cell shape, cell division, cell locomotion, and phagocytosis.[1] Filamins are actin-crosslinking proteins that give mechanical force to cells by binding to actin filaments and making the filamentous actin form bundles or gel networks.[1] Filamin is also involved in various cellular processes by anchoring transmembrane receptors such as β-integrins and scaffolding signaling molecules of diverse functions.[1,2] In human, there are three genes, *FLNA*, *FLNB*, and *FLNC* for their encoded protein, filamin A, B, and C (FLNa, FLNb, and FLNc), respectively. *FLNA* and *FLNB* are expressed ubiquitously and *FLNC* is expressed in skeletal and cardiac muscle specifically.[3,4] Mutations in human filamin genes are associated with developmental regression and defective neuronal migration.[5,6] Periventricular disease in which cerebral cortical neurons fail to migrate and oto-palato-digital (OPD) spectrum disorders that show symptoms such as cleft palate, facial malformation, and bone dysplasia are caused by mutation of *FLNA*.[7–10]

Vertebrate filamin is a dimeric protein of V-shape and each 280 kDa subunit has one actin binding domain, 24 repeating homologous rod domains, and two hinge regions.[1] Each rod domain has an immunoglobulin-like (I_g-like) folding that contains β-strands forming sandwiches of β-sheets.[11] Actin binding domain has two calponin homology (CH1 and CH2) domains and allows filamins to cross-link filamentous actin into gels.[12] First hinge region connects domains 15 with 16, and the second hinge that is a stretch of 35 amino acids in all vertebrates connects domains 23 with 24.[1] Structures of various domains of each isoform have been reported. The complex structure of FLNa domain 21 and peptide from integrin β cytoplasmic tail shows that the peptide binds to the β-strands C and D of filamin domain.[13] Complex structure of FLNa domain 17 (FLNa17) and glycoprotein Ibα (GP Ibα) tail also shows that the binding partner interacts with filamin similarly.[14] Structure of FLNc domain 24 (FLNc24) revealed how dimerization is formed in the carboxy terminal of filamin.[15] From these structures, it is suggested that the face consisting of strands C and D of filamin domains might be the general interaction site with other ligands.[13]

Here, we report the structure of FLNa domain 24 (FLNa24), compare the structure with FLNc24, and discuss how dimerization is formed in FLNa24.

Grant sponsor: Korea Science and Engineering Foundation (KOSEF); Grant number: RO1-2007-000-20275-0; Grant sponsor: 2007 BK21 Project for Pharmacy.

[†]Min-Duk Seo and Seung-Hyeon Seok contributed equally to this work.

Ae-Ran Kwon's current address is Department of Herbal Skin Care, Daegu Hanny University, Gyeongsan 712-715, Korea.

*Correspondence to: Bong-Jin Lee, Research Institute of Pharmaceutical Sciences, College of Pharmacy, Seoul National University, Seoul 151-742, Korea.
E-mail: lbj@nmr.snu.ac.kr

Received 30 July 2008; Revised 7 November 2008; Accepted 12 November 2008
Published online 24 November 2008 in Wiley InterScience (www.interscience.wiley.com). DOI: 10.1002/prot.22336

METHODS

Protein expression and purification

The open reading frame (ORF) of FLNa24 (residues 2559–2647) was cloned into the expression vector pGEX-4T-1 and was expressed in the *Escherichia coli* BL21 (DE3) strain. The cloned FLNa24 was expressed as fusion proteins with 26 kDa glutathione S-transferase (GST). Cells were grown at 20°C until an OD_{600} of 0.6 and then induced with 0.5 m*M* IPTG for 24 h. The protein was purified using GST column, GSTPrep™ FF 16/10 (GE Healthcare Bio-Science), and thrombin protease was added (20 units of thrombin per mg of protein) and incubated for 20 h at 20°C to cleave the GST tag off. After cleavage, the GST tag was separated from target protein using GST column, Glutathione Sepharose™ 4 Fast Flow (GE Healthcare Bio-Science). The purified fractions were pooled and dialyzed into 50 m*M* sodium phosphate, pH 8.0, containing 1 m*M* EDTA, 1 m*M* DDT, 1 m*M* PMSF, and 0.5 m*M* sodium azide. The dialyzed sample was applied to anion exchange column, HiPrep™ 16/10 Q FF (GE Healthcare Bio-Science) and eluted with a linear gradient from 0 to 500 m*M* NaCl in 50 m*M* sodium phosphate, pH 8.0. The purified fractions were analyzed by SDS-PAGE and concentrated by ultrafiltration using Amicon® Ultra. The concentrated sample was applied to gel filtration on Superdex™ 75 (GE Healthcare Bio-Science) with final buffer (50 m*M* Tris-HCl, pH 8.0, 100 m*M* NaCl, 1 m*M* EDTA).

Crystallization

Crystals of purified FLNa24 protein were grown by hanging drop vapor diffusion method at 20°C after mixing equal volumes (2 μL) of protein solution (30 mg/mL in final buffer) and the reservoir solution. Block shaped crystals appeared in 3–5 days in optimized reservoir solution consisting of 30% PEG3350, 0.1*M* Tris pH 8.2, and 0.2*M* lithium sulfate. For data collection, crystals were equilibrated in 20% glycerol cryo-protective solutions containing reservoir buffer and flash frozen in liquid nitrogen.

X-ray diffraction data collection and structure determination

Diffraction data were acquired at 100K on the beamline 4A at the Pohang Light Source (PLS) in Korea. Diffraction images were taken at 1° oscillation for 360° and 180 image frames were used for data processing. The data set was processed using HKL2000[16] and the CCP4 suite of programs.[17] Structure determination was performed by molecular replacement using the previously known human FLNc24 structure as a search model (PDB ID code: 1V05)[15] with the program Phaser.[18] CHAINSAW program in the CCP4 was used to mutate the search model into FLNa24 PDB file.[19] Structure refinement and rebuilding were performed by the programs CNS,[20] Refmac5[21] in CCP4, and Coot.[22] Refinement was performed using all reflections in 50–1.65Å resolution shell leaving 5% of reflections for R_{free} calculation. Rigid body refinement yielded R_{work} and R_{free} 45.3 and 44.7%, respectively. Refinement of structure was done using simulated annealing, individual B-factor refinement, and minimization implementing bulk solvent correction on all stages. Noncrystallographic symmetry (NCS) was implemented over two monomers with the restraint weight of 300 kcal/mole/Å^2. Model adjustment and refinement were done iteratively, and R_{work} and R_{free} dropped to 30.3 and 31.9%, respectively. At this stage water molecules were picked and model was refined, and R_{work} and R_{free} dropped to 24.5 and 27.3%, respectively. Two sulfate ions (from the crystallization condition) were placed in extra electron density, and model was adjusted and refined. After this stage NCS restraint was released

Table I
Data Collection and Refinement Statistics

Data collection	
Beamline	PLS BL4A
Wavelength (Å)	1.0
Space group	$P2_12_12$
Cell dimension (Å)	
	$a = 57.75$
	$b = 94.57$
	$c = 40.95$
	$\alpha = \beta = \gamma = 90.0^\circ$
Resolution (Å)	50–1.65
R_{merge}[a] (%)	5.4 (33.2)[b]
I/σ (I)	31.7 (3.6)[b]
Redundancy[c]	6.2 (5.7)[b]
Completeness (%)	97.5 (99.3)[b]
Unique reflections	27,127 (2703)[b]
Refinement	
R_{work}[d] (%)	19.2
R_{free}[e] (%)	21.9
No. atoms	
Protein	1,364
Water	184
B factor(Å^2)	
Protein	16.4
Water	30.8
Sulfate ion	36.4
RMSD[f]	
Bond lengths (Å)	0.010
Bond angles (°)	1.3
Ramachandran plot (%)	
Favorable region	90.4
Allowed region	8.9
Generously allowed region	0.7
Disallowed region	0.0
PDB accession code	3CNK

[a] $R_{merge} = \sum(I - \langle I \rangle) / \sum\langle I \rangle$.
[b] The values in parentheses indicate the highest resolution shell.
[c] N_{obs}/N_{unique}.
[d] $R_{work} = \sum_{hkl} ||F_{obs}| - k\,|F_{calc}|| / \sum_{hkl} |F_{obs}|$.
[e] R_{free} was calculated same way as R_{work}, but with the 5% of the reflections excluded from the refinement.
[f] Root mean square deviation (RMSD) was calculated with REFMAC.[21]

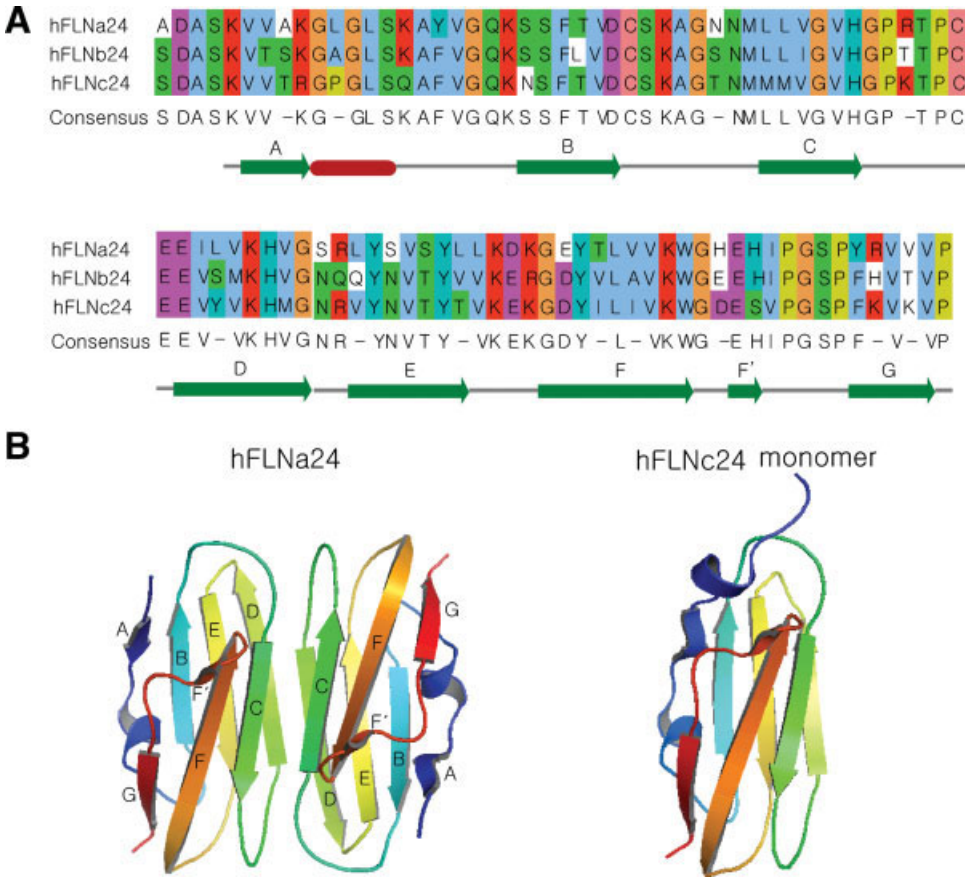

Figure 1

Protein sequences and cartoon representation of domain 24 of filamins. **A**: Multiple sequence alignment of domain 24 of human filamin A, B, and C (hFLNa24, hFLNb24, and hFLNc24). Sequence alignment was generated by CLUSTALW[25] and was colored by default according to the ClustalX coloring scheme.[26] Secondary structure elements of FLNa24 are shown below the sequences. **B**: Cartoon representation of hFLNa24 and hFLNc24. Left: dimeric structure of hFLNa24, right: monomeric structure of hFLNc24. Figures were generated using PyMOL.[27]

and refinement was done, yielding R_{work} and R_{free} values of 21.4 and 23.8%, respectively. Model was adjusted and refined further in CCP4 using Refmac5. Finally, Refmac refinement with TLS refinement[23] resulted in R_{work} and R_{free} values of 19.2 and 21.9%, respectively.

The final model had R_{work} and R_{free} of 19.2 and 21.9%, respectively. The data collection and refinement statistics are summarized in Table I. The final structure was verified using PROCHECK[24] and all the residues were in the most favorable region, additionally allowed region, or generously allowed region of the Ramachandran plot. The atomic structure and structure factor were deposited with the PDB ID code 3CNK.

RESULTS AND DISCUSSION

Overall structure of the FLNa24 forms immunoglobulin-like fold (see Fig. 1). Strands A, B, E, and D form a β-sheet and strands C, F, and G form another β-sheet. A dimer is in the asymmetric unit and the RMSD of the two monomers is 0.3Å. The noticeable differences in main chain between the two monomers lie in six regions. These are in residues 2565–2566 (in helix), 2578–2580 (in β-strand B), 2595–2597 (in loop CD), 2610–2613 (in β-strand D and loop DE), 2622–2624 (in loop EF), and 2645–2647 (in the C-terminus). As it can be predicted from high sequence identity (69.7 and 67.4% for FLNb and FLNc, respectively), the structure is very similar to the structure of the same domain of FLNb (PDB code 2EED) and FLNc (see Fig. 1).[15] The root mean square deviation (RMSD) between FLNa24 and FLNc24 is only 0.6Å (Table II). The RMSD between the dimers of FLNa24 and FLNc24 is 0.7Å. The difference in secondary structure between FLNa24 and FLNc24 lies only in the length of strand D. Strand D of FLNa24 has eight amino acids (Glu2603-Gly2610) and its amino acid length is two amino acids longer than that of FLNc24. RMSD value between FLNb24 and FLNc24 is 1.2Å with 70.5% sequence identity. Considering the small RMSD between

Table II
Root Mean Square Deviation (RMSD) Values for the Structures Superposed on Domain 24 of Filamin A

Domain	RMSD (Å)	PDB entry
Gelation factor domain 4	1.3	1WLH
Gelation factor domain 5	1.4	1QFH
Gelation factor domain 6	1.5	1QFH
Filamin A domain 17	1.1	2BP3
Filamin A domain 19	1.1	2J3S
Filamin A domain 21	0.9	2BRQ
Filamin B domain 24	1.2	2EED
Filamin C domain 14	1.7	2D7M
Filamin C domain 16	2.7	2D7N
Filamin C domain 17	2.4	2D7O
Filamin C domain 22	2.1	2D7P
Filamin C domain 23	1.0	2NQC
Filamin C domain 24	0.6	1V05

RMSD values are obtained using secondary-structure matching (SSM) Superpose tool[28] in the program Coot.[22] For RMSD comparison, one monomer (chain A) was used if coordinates contain a dimer, and in the case of NMR ensembles, the best representing structure was used. The choice of PDB entry used by Sjekloća *et al.*[29] was adopted for gelation factor domains.

FLNa24 and FLNc24, it is interesting to see the result of Himmel *et al.*[30] that FLNa does not form dimer with other filamin isoforms while FLNb and FLNc may form heterodimer. Sjekloca *et al.*[29] compared the structure of the domain 23 of FLNc with those of other similar immunoglobulin domains and showed that the structure has high structural similarity to domain 17 of FLNc and domain 21 of FLNa. When the structure of FLNa24 is compared with those of other similar immunoglobulin domains, it shows high structural similarity to the domain 23 of FLNc and domains 17, 19, and 21 of FLNa among other nondimerizing domains (Table II).

The interface between two monomers in dimer structure of FLNa24 is formed by mainly strands C and D as shown in FLNc24 structure [Fig. 1(B)]. It is very similar to the dimerization interface of FLNc24 in its size, the characteristics of composing amino acid residues, and dimerization pattern.[15] The interface buries 18% (977Å^2) of the solvent accessible surface of the monomer. The interface (Asn2857-Gly2610) contains 42% of polar amino acids and strand D region contains more polar residues than stand C region does. Putative hydrogen bond formation between the two C strands and that between the two D strands is distinctive [Fig. 2(A,B)]. There are six hydrogen bondings between the main chains of the two D strands, and five water molecules connect the two D strands through hydrogen bonding in

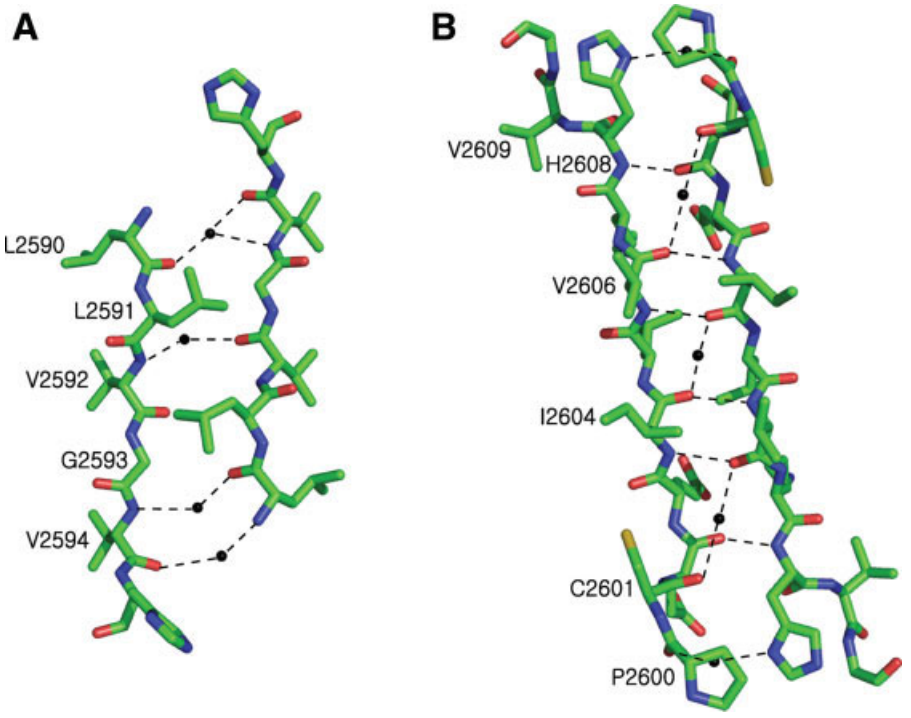

Figure 2
Dimerization interface of domain 24 of filamin A. **A**: Hydrophobic interaction and putative hydrogen bonding between the two C strands. Hydrophobic stacking is formed by residues Leu2591, Val2592, and Gly2593. Interaction between the two C strands is featured by this hydrophobic interaction as it is revealed in domain 24 of filamin C by Pudas *et al.*[15] Four water molecules are involved in the hydrogen bonding network. **B**: Putative hydrogen bonding network between the two D strands. There are six hydrogen bondings between protein residues, and additionally five water molecules are involved in the hydrogen bonding network. Figure 2(A,B) was generated using PyMOL. For clarity, protein residues are shown as sticks and water molecules are represented as black spheres.

addition. The number of hydrogen bonding between the main chains of the two C strands in FLNa24 is same as that in FLNc24. Strand Cs form no direct hydrogen bonding between two monomers but four water molecules are involved in hydrogen bonding network. Instead, three residues (Leu2591, Val2592, and Gly2593) of the strand C are contributing to the hydrophobic interaction between two monomers. It is interesting to see that dimerization of domain 24 is formed by antiparallel association of each domain. It is speculated that the hinge region, which flanks the domain 24, gives room for the domain 24 region to be flexible so that the dimerization domains form antiparallel structure while other rod domains of whole filamin dimer run parallely along the filamin rod axis.

The interaction of filamin with other proteins is regulated by different mechanism such as receptor occupancy, phosphorylation, and proteolysis.[2] The potential phosphorylation sites for the 11 domains of FLNc were reported previously as the conserved three residues, (Ser, Phe) Pro (Phe, Tyr, Thr).[29] The putative phosphorylation site, Ser2640-Pro2641-Tyr2642 is also found in carboxy terminus of FLNa24.

Different binding partners interact with domain 24 or tandem domains including domain 24 of filamins. Domain 21–24 of filamin can interact with various proteins including presenilins.[31] Domain 24 of FLNa interacts with the small GTPase RalA[32] and Granzyme B.[33] For the human FLNc, domain 24 alone is enough and sufficient for dimerization.[29] In FLNa24 structure, strands C and D are forming dimerization interface as previously shown in FLNc24 structure.[15] Interestingly, in the complex structure of FLNa17 and GPIbα, it was the strands C and D of FLNa17 that were interacting with the GPIbα peptide.[14] These show that domain 24 may have a role in interaction with other binding molecules in addition to the dimerization role. Elucidating how domain 24 interacts with other binding partners and which part of domain 24 is involved would give further information on the features of the residues of FLNa that are involved in the interaction.

ACKNOWLEDGMENTS

We thank the Korea Basic Science Institute (KBSI) and the National Center for Inter-University Research Facilities (NCIRF) at Seoul National University for the use of NMR spectrometers.

REFERENCES

1. Stossel TP, Condeelis J, Cooley L, Hartwig JH, Noegel A, Schleicher M, Shapiro SS. Filamins as integrators of cell mechanics and signalling. Nat Rev Mol Cell Biol 2001;2:138–145.
2. van der Flier A, Sonnenberg A. Structural and functional aspects of filamins. Biochim Biophys Acta 2001;1538:99–117.
3. Gorlin JB, Yamin R, Egan S, Stewart M, Stossel TP, Kwiatkowski DJ, Hartwig JH. Human endothelial actin-binding protein (ABP-280, nonmuscle filamin): a molecular leaf spring. J Cell Biol 1990; 111:1089–1105.
4. Thompson TG, Chan YM, Hack AA, Brosius M, Rajala M, Lidov HG, McNally EM, Watkins S, Kunkel LM. Filamin 2 (FLN2): a muscle-specific sarcoglycan interacting protein. J Cell Biol 2000; 148:115–126.
5. Feng Y, Chen MH, Moskowitz IP, Mendonza AM, Vidali L, Nakamura F, Kwiatkowski DJ, Walsh CA. Filamin A (FLNA) is required for cell-cell contact in vascular development and cardiac morphogenesis. Proc Natl Acad Sci USA 2006;103:19836–19841.
6. Masruha MR, Caboclo LO, Carrete H, Jr, Cendes IL, Rodrigues MG, Garzon E, Yacubian EM, Sakamoto AC, Sheen V, Harney M, Neal J, Sean Hill R, Bodell A, Walsh C, Vilanova LC. Mutation in filamin A causes periventricular heterotopia, developmental regression, and West syndrome in males. Epilepsia 2006;47:211–214.
7. Dudding BA, Gorlin RJ, Langer LO. The oto-palato-digital syndrome. A new symptom-complex consisting of deafness, dwarfism, cleft palate, characteristic facies, and a generalized bone dysplasia. Am J Dis Child 1967;113:214–221.
8. Fox JW, Lamperti ED, Eksioglu YZ, Hong SE, Feng Y, Graham DA, Scheffer IE, Dobyns WB, Hirsch BA, Radtke RA, Berkovic SF, Huttenlocher PR, Walsh CA. Mutations in filamin 1 prevent migration of cerebral cortical neurons in human periventricular heterotopia. Neuron 1998;21:1315–1325.
9. Poussaint TY, Fox JW, Dobyns WB, Radtke R, Scheffer IE, Berkovic SF, Barnes PD, Huttenlocher PR, Walsh CA. Periventricular nodular heterotopia in patients with filamin-1 gene mutations: neuroimaging findings. Pediatr Radiol 2000;30:748–755.
10. Robertson SP, Twigg SR, Sutherland-Smith AJ, Biancalana V, Gorlin RJ, Horn D, Kenwrick SJ, Kim CA, Morava E, Newbury-Ecob R, Orstavik KH, Quarrell OW, Schwartz CE, Shears DJ, Suri M, Kendrick-Jones J, Wilkie AO. Localized mutations in the gene encoding the cytoskeletal protein filamin A cause diverse malformations in humans. Nat Genet 2003;33:487–491.
11. Feng Y, Walsh CA. The many faces of filamin: a versatile molecular scaffold for cell motility and signalling. Nat Cell Biol 2004;6:1034–1038.
12. Nakamura F, Hartwig JH, Stossel TP, Szymanski PT. Ca^{2+} and calmodulin regulate the binding of filamin A to actin filaments. J Biol Chem 2005;280:32426–32433.
13. Kiema T, Lad Y, Jiang P, Oxley CL, Baldassarre M, Wegener KL, Campbell ID, Ylanne J, Calderwood DA. The molecular basis of filamin binding to integrins and competition with talin. Mol Cell 2006;21:337–347.
14. Nakamura F, Pudas R, Heikkinen O, Permi P, Kilpelainen I, Munday AD, Hartwig JH, Stossel TP, Ylanne J. The structure of the GPIb-filamin A complex. Blood 2006;107:1925–1932.
15. Pudas R, Kiema TR, Butler PJ, Stewart M, Ylanne J. Structural basis for vertebrate filamin dimerization. Structure 2005;13:111–119.
16. Otwinowski Z, Minor W. Processing of X-ray diffraction data collected in oscillation mode. Methods Enzymol 1997;276:307–326.
17. Collaborative Computational Project, Number 4. The CCP4 suite: programs for protein crystallography. Acta Crystallogr D Biol Crystallogr 1994;50(Pt 5):760–763.
18. McCoy AJ. Solving structures of protein complexes by molecular replacement with Phaser. Acta Crystallogr D Biol Crystallogr 2007; 63(Pt 1):32–41.
19. Stein N. CHAINSAW: a program for mutating pdb files used as templates in molecular replacement. J Appl Cryst 2008;41:641–643.
20. Brunger AT, Adams PD, Clore GM, DeLano WL, Gros P, Grosse-Kunstleve RW, Jiang JS, Kuszewski J, Nilges M, Pannu NS, Read RJ, Rice LM, Simonson T, Warren GL. Crystallography and NMR system: a new software suite for macromolecular structure determination. Acta Crystallogr D Biol Crystallogr 1998;54(Pt 5):905–921.

21. Murshudov GN, Vagin AA, Dodson EJ. Refinement of macromolecular structures by the maximum-likelihood method. Acta Crystallogr D Biol Crystallogr 1997;53(Pt 3):240–255.
22. Emsley P, Cowtan K. Coot: model-building tools for molecular graphics. Acta Crystallogr D Biol Crystallogr 2004;60(Pt 12 Pt 1): 2126–2132.
23. Winn MD, Murshudov GN, Papiz MZ. Macromolecular TLS refinement in REFMAC at moderate resolutions. Methods Enzymol 2003; 374:300–321.
24. Laskowski RA, MacArthur MW, Moss DS, Thornton JM. PROCHECK: a program to check the stereochemical quality of protein structures. J App Crystallogr 1993;26:283–291.
25. Thompson JD, Higgins DG, Gibson TJ. CLUSTAL W: improving the sensitivity of progressive multiple sequence alignment through sequence weighting, position-specific gap penalties and weight matrix choice. Nucleic Acids Res 1994;22:4673–4680.
26. Thompson JD, Gibson TJ, Plewniak F, Jeanmougin F, Higgins DG. The CLUSTAL_X windows interface: flexible strategies for multiple sequence alignment aided by quality analysis tools. Nucleic Acids Res 1997;25:4876–4882.
27. DeLano WL. The PyMOL molecular graphics system. San Carlos, CA: DeLano Scientific; 2002. Available at: http://www.pymol.org.
28. Krissinel E, Henrick K. Secondary-structure matching (SSM), a new tool for fast protein structure alignment in three dimensions. Acta Crystallogr D Biol Crystallogr 2004;60(Pt 12 Pt 1):2256–2268.
29. Sjekloca L, Pudas R, Sjoblom B, Konarev P, Carugo O, Rybin V, Kiema TR, Svergun D, Ylanne J, Djinovic Carugo K. Crystal structure of human filamin C domain 23 and small angle scattering model for filamin C 23-24 dimer. J Mol Biol 2007;368:1011–1023.
30. Himmel M, van Der Ven PF, Stocklein W, Furst DO. The limits of promiscuity: isoform-specific dimerization of filamins. Biochemistry 2003;42:430–439.
31. Zhang W, Han SW, McKeel DW, Goate A, Wu JY. Interaction of presenilins with the filamin family of actin-binding proteins. J Neurosci 1998;18:914–922.
32. Ohta Y, Suzuki N, Nakamura S, Hartwig JH, Stossel TP. The small GTPase RalA targets filamin to induce filopodia. Proc Natl Acad Sci USA 1999;96:2122–2128.
33. Browne KA, Johnstone RW, Jans DA, Trapani JA. Filamin (280-kDa actin-binding protein) is a caspase substrate and is also cleaved directly by the cytotoxic T lymphocyte protease granzyme B during apoptosis. J Biol Chem 2000;275:39262–39266.